Chinese Journal of Chemistry, **2004**, *22*, 232—237 **Article**

$Li_3AlB_2O_6$: Synthesis, Crystal Structure, and Its Luminescence Property Compared with $LiSrBO_3$

WANG, Hai-Xia(王海侠) CHENG, Wen-Dan*(程文旦) CHEN, Da-Gui(陈达贵)
ZHANG, Hao(张浩) WU, Dong-Sheng(吴东升) GONG, Ya-Jin(龚亚京)

Fujian Institute of Research on the Structure of Matter, the Graduate School of Chinese Academy of Sciences, State Key Laboratory of Structural Chemistry, Fuzhou, Fujian 350002, China

The synthesis and crystal structure of $Li_3AlB_2O_6$ with different cell parameters are reported and these cells are transformed each other from the confirmation of crystallographic structural analyses. The absorption spectrum, luminescence and lifetimes of the $Li_3AlB_2O_6$ and $LiSrBO_3$ solid compounds are measured and the comparisons are made between them. It is shown that the absorption edges are at about 400 nm (or band gap 3.1 eV) and there is one of absorption peaks at about 350 nm for the $Li_3AlB_2O_6$ and $LiSrBO_3$. The emission band (530 nm) makes a red shift and fluorescence decay time (24.39 ns) of the $Li_3AlB_2O_6$ becomes smaller compared with the emission band (480 nm) and lifetime (93.16 ns) of the $LiSrBO_3$ at the visible region. The transition energies and oscillator strengths of the clusters $(Li_3AlB_2O_6)_2$ and $(LiSrBO_3)_2$ lying at low excited states are calculated by the time-dependent Hartree-Fock method. The obtained results are used to model the photophysical properties and discuss the origin of spectral bands of the $Li_3AlB_2O_6$ and $LiSrBO_3$.

Keywords synthesis, crystal structure, photoluminescence properties

Introduction

In the past ten years, the chemistry of borates including oxyborates, hydroxide borates and fluoride borates has been reinvestigated, mainly due to its applications as optical materials, such as second harmonic generation[1,2] and host materials for fluorescence.[3,4] Among the binary systems, β-BaB_2O_4 (BBO)[1] and LiB_3O_5[2] have been commonly applied to nonlinear optical materials. In the recent years the ternary systems have been also investigated in order to find new nonlinear optical materials with good properties.[5] For examples, $CsLiB_6O_{10}$ (CLBO) crystal[6] possesses a smaller walk-off angle and larger angular, spectral and temperature bandwidths than BBO, and produces high-power deep-UV light. $K_2Al_2B_2O_7$ (KAB) crystal has a cutoff wavelength down to 180 nm.[7] The basic structural features of the KAB crystal are K^+ cations, $(BO_3)^{3-}$ triangles and distorted $(AlO_4)^{5-}$ tetrahedron. Generally, a large distortion and inhomogeneous electronic density distribution will lead to a great second-order microscopic susceptibility. Accordingly, Al atom seems to be a good candidate on account of its commonly tetra-coordinated environment and easily polarized electronic distribution compared with B atom. In order to synthesize new borates and search for new optical materials, recently, He, M. and coworkers have studied the phase relations in the Li_2O-Al_2O_3-B_2O_3 ternary system including six compounds,[8] among which the crystals of $Li_2AlB_5O_{10}$, $Li_2Al_2B_4O_{10}$, $Li_3AlB_2O_6$ and $LiAl_7B_4O_{17}$ were structurally characterized. Abdullaev and coworkers[9,10] first found the compound $Li_3AlB_2O_6$ in 1974 and refined it in 1982. However, He, M. and coworkers obtained this structure[11] which was different from the one reported by Abdullaev *et al.*[9,10] Moreover, great efforts have been done to research borate doped rare-earth or transition metal cations. A sensitized or an activated cation is added to borate making optical emission from ultraviolet to red region.[12,13]

In order to explore a promising photoluminescence material from the borate crystals with non-dopants, the compound $Li_3AlB_2O_6$ was synthesized by the solid state reaction and the single crystal structure was determined. We obtain the cell parameters that are reducible, and find that the two separate cells transformed each other can obtain the same structure. In addition, its luminescence properties were investigated and compared with those of the crystal $LiSrBO_3$[14]. From the observed results we found that fluorescence spectrum has a red shift about 50 nm for the $Li_3AlB_2O_6$ compared with $LiSrBO_3$ in a green-visible region. At the same time, the time-dependent Hartree-Fock (TDHF) method was employed to calculate the transition energies and oscillator strengths in order to explain the origin of luminescence from the borate self-system not from the doped system.

* E-mail: cwd@ms.fjirsm.ac.cn
Received May 19, 2003; revised and accepted November 1, 2003.
Project supported by the National Science Foundation of China (No. 90201015), the Science Foundation of the Fujian Province (No. E0210028), and the Foundation of State Key Laboratory of Structural Chemistry (No. 030060).

Experimental and computational procedures

Synthesis and crystal growth of $Li_3AlB_2O_6$

A mixture containing appropriate amounts of Li_2CO_3 (Chemical pure), $Al(OH)_3$ (Chemical pure), and H_3BO_3 (Analytical reagent) was ground into fine powder in a mortar of agate, transferred to a platinum crucible and calcined at 773 and 983 K. The sinter was continually heated to 1013 K and kept at this temperature for 24 h, after experiencing a few grindings. The temperature was slowly cooled from 1013 to 873 K, finally to room temperature. A few colorless prism crystals were found from the melt of the mixture.

X-ray determination

A single crystal of $Li_3AlB_2O_6$ with approximate dimensions of 0.25 mm×0.05 mm×0.15 mm was selected for single-crystal X-ray diffraction. The diffraction data were collected on an Enraf-Nonius CAD4 diffractometer with graphite monochromator Mo Kα radiation (λ=0.071073 nm). The intensity data were collected using the $\omega/2\theta$ scan technique. 716 unique reflections of the 2974 reflections were used in the structural determination and refinement after the empirical absorption correction (ψ-scan). The structure was solved anisotropically with SHELXS-97 program package[15,16] and refined by full-matrix least-squares converged to R_1 =0.0379 for 654 $F_o > 4\sigma(F_o)$ and 0.0530 for all 716 data. $wR_2 = 0.1256$, (in which $w = 1/[\sigma^2(F_o^2) + (0.1111*P)^2 + 0.11*P]$, where $P = (\mathrm{Max}(F_o^2, 0) + 2*F_c^2)/3$). The refinement details and the crystal data are listed in Table 1. The final atomic coordinates and isotropic displacement parameters are given in Table 2. Selected bond distances and angles are listed in Table 3. Aluminum positions were determined by direct methods in space group $P\bar{1}$. The remaining oxygen, boron and lithium positions were found in subsequent difference Fourier maps. Here, all data of the $Li_3AlB_2O_6$ compound can be indexed on the reduced cell which were transferred from original cell with a=0.48887(10) nm, b = 0.617150(10) nm, c = 0.78885(10) nm, α = 74.47(3)°, β=89.54(3)°, γ=89.70(1)°. Additionally, the original cell with lattice parameters a=0.617150(10) nm, b=0.48887(10) nm, c=0.78885(10) nm, α= 90.45(7)°, β=105.52(7)°, γ=89.70(1)° was also tried in terms of the suggested space $P\bar{1}$. After refining by the full-matrix least-squares (shelx97), final structure factors for this in $P\bar{1}$: R_1=0.0380 for 654 $F_o > 4\sigma(F_o)$ and 0.0529 for all 716 data. Accordingly, using triclinic $P\bar{1}$ space group, we can obtain the same structure from the original cell and reduced cell parameters.

Spectrum measurement

The absorption spectroscopy measurements were carried out with Cary 500 instrument Ver. 8.01, which can be converted to corresponding derivative spectrum. The luminescence spectra were recorded using a He-Cd 325 nm laser as the excitation source. The nanosecond lifetimes were obtained by exciting at 397 nm using Edinburgh Analytical Instruments F900 with the scan type of exponential fit time scan at room temperature. The samples were prepared from pressed abradant of selected micro crystals.

Table 1 Crystallographic data and refinement details

Chemical formula	$Li_3AlB_2O_6$	$Li_6Al_2B_4O_{12}$
Fw	165.42	330.84
Crystal system	Triclinic	Triclinic
Space group	$P\bar{1}$	$P\bar{1}$
a/nm	0.488870(10)	0.617150(10)
b/nm	0.617150(10)	0.488870(10)
c/nm	0.788850(10)	0.788850(10)
α/(°)	89.70(2)	90.457
β/(°)	74.473	105.527
γ/(°)	89.543	89.70(1)
V/nm^3	0.229306(7)	0.229306(7)
Z	2	1
D/(g • cm^{-3})	1.198	2.396
hkl range	$-5 \leqslant h \leqslant 5$, $-6 \leqslant k \leqslant 7$, $0 \leqslant l \leqslant 9$	$-5 \leqslant h \leqslant 5$, $-6 \leqslant k \leqslant 7$, $-9 \leqslant l \leqslant 0$
R_1	0.0379	0.0380
wR_2	0.1256	0.1282
S	1.314	0.997

Table 2 Fractional atom coordinates and equivalent isotropic displacement parameters

Atom	*x*	*y*	*z*	U_{eq}[a]
Al(1)	0.35098(17)	0.94925(15)	0.72638(12)	0.0095(5)
Li(1)	−0.1723(12)	0.5210(11)	0.2562(8)	0.0245(14)
Li(2)	0.1653(11)	0.7616(9)	0.3900(7)	0.0151(12)
Li(3)	0.3212(11)	0.6113(10)	1.0734(7)	0.0208(13)
B(1)	0.3418(7)	1.3202(6)	0.4294(5)	0.0101(8)
B(2)	0.8345(7)	0.8282(6)	0.9093(5)	0.0108(8)
O(1)	0.3896(4)	0.7439(4)	0.6055(3)	0.0119(6)
O(2)	0.2097(4)	0.4901(4)	0.3194(3)	0.0121(6)
O(3)	0.1201(4)	0.8377(4)	0.8940(3)	0.0121(6)
O(4)	0.2258(4)	1.2046(4)	0.5897(3)	0.0128(6)
O(5)	0.6875(4)	0.9888(4)	0.7843(3)	0.0123(6)
O(6)	0.7094(5)	0.6670(4)	1.0308(3)	0.0136(7)

[a] $U_{eq} = 1/3\Sigma_i\Sigma_j U_{ij}\alpha^*_i\alpha^*_j\alpha_i\alpha_j$.

Computational procedures

The transition energies and oscillator strengths of cluster $(Li_3AlB_2O_6)_2$ and $(LiSrBO_3)_2$ were calculated from ground state to singlet excited states by the time dependent Hartree-Fock (TDHF) method at CEP-31G

Table 3 Selected interatomic distances (10^{-1} nm) and angles (°)

Al(1)—O(3)	1.730(2)	Li(2)—O(5)[a]	1.909(6)
Al(1)—O(5)	1.747(2)	Li(2)—O(2)	1.913(6)
Al(1)—O(4)	1.764(2)	Li(2)—O(4)[c]	1.932(6)
Al(1)—O(1)	1.787(2)	Li(2)—O(1)	2.008(6)
Li(1)—O(6)[d]	1.861(6)	Li(3)—O(6)	1.941(6)
Li(1)—O(2)	1.931(6)	Li(3)—O(2)[e]	1.958(6)
Li(1)—O(1)[b]	2.009(7)	Li(3)—O(3)	1.967(6)
Li(1)—O(4)[c]	2.346(8)	Li(3)—O(6)[f]	2.100(7)
B(1)—O(2)[g]	1.336(4)	B(2)—O(6)	1.330(4)
B(1)—O(4)	1.393(4)	B(2)—O(5)	1.397(4)
B(1)—O(1)[a]	1.415(4)	B(2)—O(3)[h]	1.401(4)
O(3)-Al(1)-O(5)	117.88(11)	O(2)10-B(1)-O(4)	121.1(3)
O(3)-Al(1)-O(4)	110.47(11)	O(2)10-B(1)-O(1)[a]	122.3(3)
O(5)-Al(1)-O(4)	108.86(11)	O(4)-B(1)-O(1)[a]	116.5(3)
O(3)-Al(1)-O(1)	106.08(11)	O(6)-B(2)-O(5)	121.7(3)
O(5)-Al(1)-O(1)	102.48(11)	O(6)-B(2)-O(3)[h]	121.6(3)
O(4)-Al(1)-O(1)	110.67(11)	O(5)-B(2)-O(3)[h]	116.6(3)

Symmetry transformations used to generate equivalent atoms: a, $-x+1$, $-y+2$, $-z+1$; b, $-x$, $-y+1$, $-z+1$; c, $-x$, $-y+2$, $-z+1$; d, $x-1$, y, $z-1$; e, x, y, $z+1$; f, $-x+1$, $-y+1$, $-z+2$; g, x, $y+1$, z; h, $x+1$, y, z.

basis set level[17,18] and run in program Gaussian98.[19] The SCF convergence criterion of the RMS density matrix and the maximum density matrix was set at 10^{-8} and 10^{-6}, respectively, in the excited state calculations. The iterations of excited states were continued until the changes on energies of states are no more than 10^{-7} a.u. between the iterations, and the convergence has been obtained in the all calculations of excited states. The results from the calculations of the clusters were used to model the electronic absorption spectrum of $Li_3AlB_2O_6$ and $LiSrBO_3$ solid compounds. The geometrical parameters of the clusters employed in the calculations were selected from the X-ray single crystal determinations.

Results and discussion

Crystal structure simple descriptions

Tetrahedral AlO_4, LiO_4 and plane BO_3 drawings of the structure are in Figure 1a. Elongated $[LiAlBO_3]^+$ hexagonal rings form an infinite chain along a axis connecting by the neighboring oxygen, boron atom from BO_3 or LiO_4 and the chains are crosslinked to form the sheets in two ways. First by the Al(1) atoms, each aluminium is bounded to O(3), O(5) in one chain and O(1) in another O(2) out of ring was deleted for clarity); the second type of connection is produced by the B(2) atoms. These sheets stack along *b*-axis to form the three-dimensional framework. Non-ring lithium atoms are averagely located in the channels. Displacement ellipsoid plots of the Li coordination are shown in Figure 1b, the LiO_4 chains were produced by sharing oxygen of the adjacent AlO_4 along *c*-direction. The AlO_4 tetrahedron is regular, with equal bond lengths and bond angles. The BO_3 group is close to ideal with average bond length 0.1378(6) nm being in agreement with values found in $B(OH)_3$,[20] but in one of LiO_4 tetrahedrons one bond length is larger than common Li—O length, due to configuration distortion.

Luminescence properties of $Li_3AlB_2O_6$ and $LiSrBO_3$.

The UV-vis spectra of these two species were measured and given in Figure 2. The derivative absorption spectra shown in Figure 3 do not contain more information than the normal absorption spectra but fine structural features are more readily apparent. It is found from Figure 2 that there is an absorption band at about 250

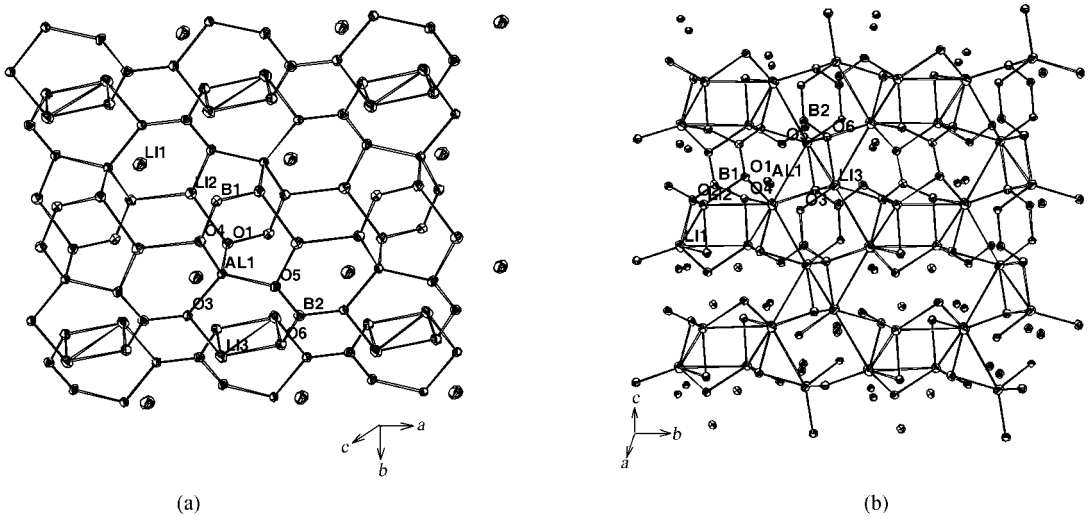

Figure 1 (a) Fundamental structure fragment of $[LiAlBO_3]^+$ showing the connection of Al cations and triagonal BO_3 groups along *a*-axis. (b) LiO_4 tetrahedron ellipsoid plots, B—O and Al—O bonds were deleted for clarity.

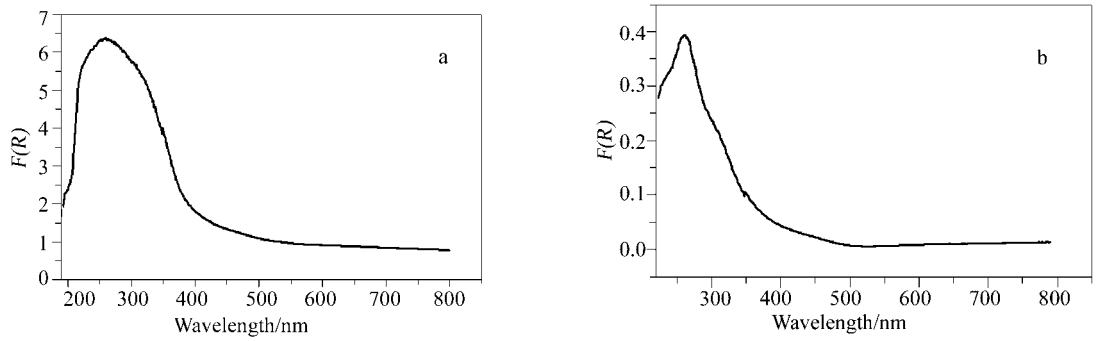

Figure 2 (a) Absorption spectra of $Li_3AlB_2O_6$ in little solid crystals and (b) absorption spectra for $LiSrBO_3$ in little solid crystals.

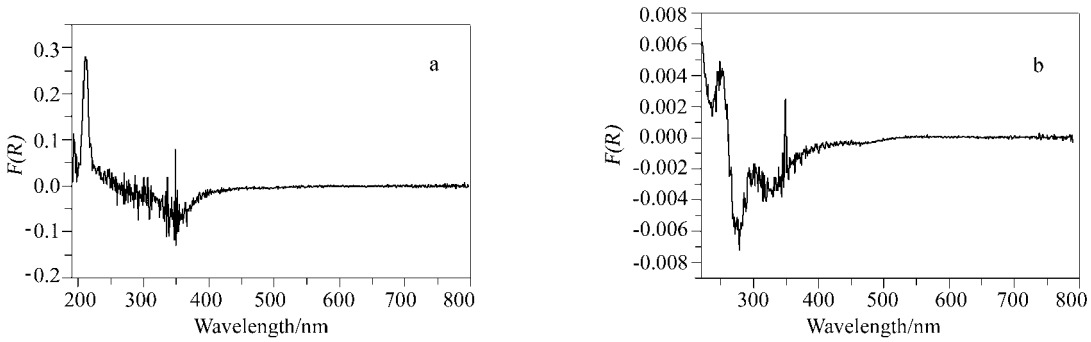

Figure 3 Profiles of derivative spectrum for (a) $Li_3AlB_2O_6$ and (b) $LiSrBO_3$.

nm and 260 nm, for $Li_3AlB_2O_6$ and $LiSrBO_3$, respectively. There are both absorption peaks at about 350 nm and absorption edge of about 400 nm for $Li_3AlB_2O_6$ and $LiSrBO_3$ observed in Figure 3. The emission spectra were determined at room temperature using 325 nm excitation wavelength in the pump-probe continuous optical output. The emissions of $Li_3AlB_2O_6$ and $LiSrBO_3$ were observed at wavelengths of about 450, 530 nm and 450, 480 nm, respectively, (see Figure 4). From the emission profiles, the bands of $Li_3AlB_2O_6$ exhibit a red shift of about 50 nm at a green-visible region. For further study, their fluorescence life decay curves were also recorded and shown in Figure 5. The excited states decay nearly exponentially with the average lifetimes of 24.39 and 93.16 ns for $Li_3AlB_2O_6$ and $LiSrBO_3$, respectively. To our knowledge, it is the first time to report the luminescence emission from solid state borate compounds of non-dopant. In the different stage of the life-decayed curves the average lifetime was calculated using the most common lifetime-decayed formula such as $I/I_0=\exp(-t/T_1)$, that is, the single exponential fits.

In order to explain the origin of spectra, we also made calculation of transition energies and oscillator strengths lying at low excited states and compared them with the measurement spectra. The transition energies and oscillate strengths of some excited states were calculated at the TDHF CEP-31G level for the $(Li_3AlB_2O_6)_2$ and $(LiSrBO_3)_2$ clusters. Table 4 lists the transition energies (corresponding to wavelengths) and oscillator strengths lying at some low excited states. Figure 6 gives relations between the oscillator strengths and absorption wavelengths at some excited states. The three excited states with the largest oscillator strengths are named as S_{l1}, S_{l2} and S_{l3}, individually. The calculated transition wavelength from singlet ground state S_0 to singlet excited state S_{l2} is separately 350 and 370 nm for the $(Li_3AlB_2O_6)_2$ and $(LiSrBO_3)_2$ clusters. These two transition wavelengths will possibly correspond to the measured peaks at about 350 nm in Figure 3, and mostly arise from transitions of O^{2-} to $(Li_2)^{2+}$ or Sr^{2+} ionic states for the $Li_3AlB_2O_6$ and $LiSrBO_3$ individually in terms of analyses from the calculated results. The absorption process occurs principally by electronic transition from the singlet ground state S_0 to the excited singlet states S_n, on the contrary, the emission occurs from the excited states S_n to S_0. Accordingly, the excited singlet state is responsible for the fluorescence processes. The observed emission band at about 450 nm will be assigned as the electron transitions from S_{l2} to S_0 states, while at about 530 and 480 nm assigned as the electron transitions from S_{l1} to S_0 states for the $Li_3AlB_2O_6$ and $LiSrBO_3$, respectively, after considering the Stokes' shift, that is, the emission band has larger wavelength than that of the absorption band. The calculated results show that the emission band from S_{l1} to S_0 states mostly originate from the charge transfers between the different environments of Li atoms for the $Li_3AlB_2O_6$, and the charge transfers from the Sr atom in excited state to LiO group for the $LiSrBO_3$. The fluorescence spectrum of the $Li_3AlB_2O_6$ (530 nm) makes a

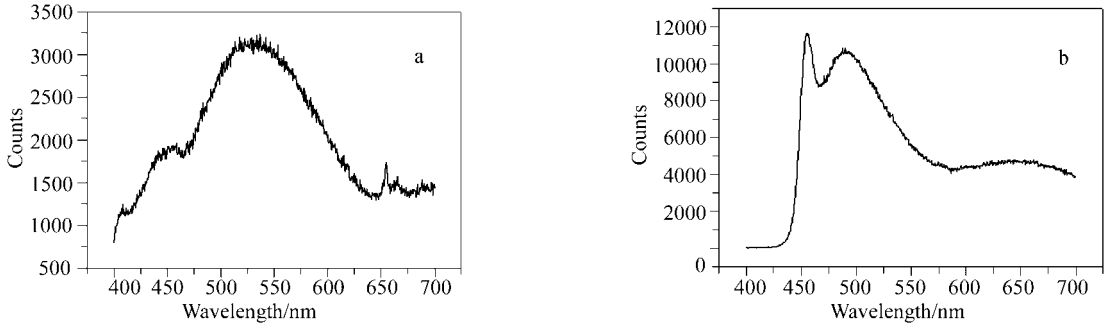

Figure 4 Room temperature emission spectra of (a) $Li_3AlB_2O_6$ and (b) $LiSrBO_3$ after a 325 nm laser excitation.

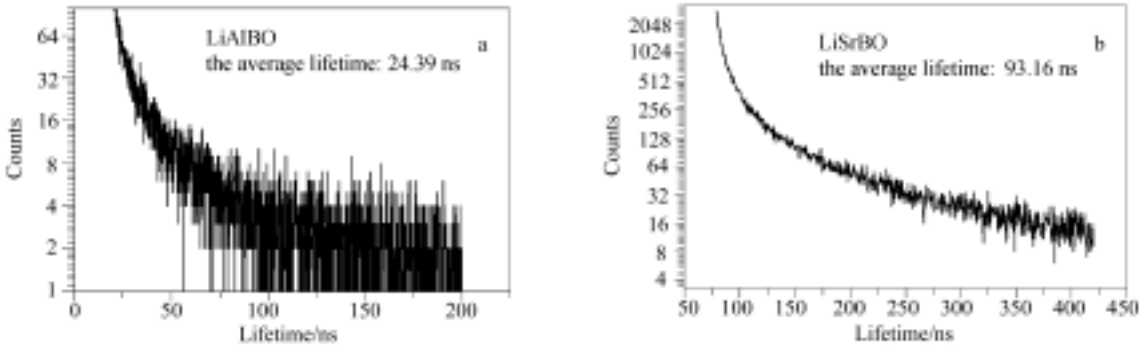

Figure 5 Green-visible region life decay curves for (a) $Li_3AlB_2O_6$ and (b) $LiSrBO_3$ at a laser excitation (397 nm, 35 ps), room temperature.

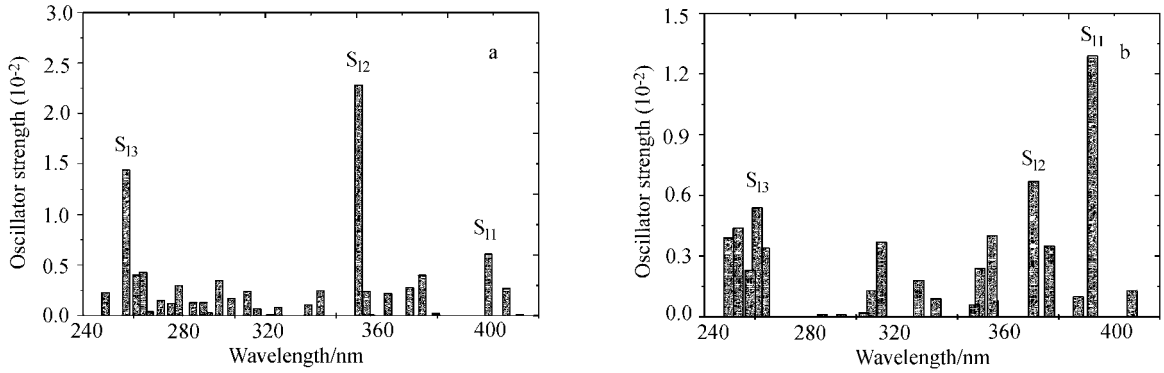

Figure 6 The calculated electronic absorption spectrum of (a) $Li_3AlB_2O_6$ and (b) $LiSrBO_3$ by the time-dependent Hartree-Fock method at basis set CEP-31G level.

red shift compared with that of the $LiSrBO_3$ (480 nm), and the observed radiative decay time is smaller for the $Li_3AlB_2O_6$ (24.39 ns) than for the $LiSrBO_3$ (93.16 ns). The calculated absorption bands S_{l3} of 257 and 261 nm will separately correspond to the measured bands of 250 and 260 nm for the $Li_3AlB_2O_6$ and $LiSrBO_3$, and arise from the mixing contributions between the charge transfers from O^{2-} to different metal ions.

Conclusions

In this work we have done three things. Firstly, the $Li_3AlB_2O_6$ compound was synthesized by solid state reaction at high temperature and its structure with different cell parameters transformed each other was determined from single-crystal X-ray diffraction. Then, the absorption spectrum, luminescence and lifetime of the $Li_3AlB_2O_6$ and $LiSrBO_3$ solid compounds are measured. Three absorption peaks from ultraviolet to visible were observed and the transmittance cutoff at about 400 nm in visible (or band gap 3.1 eV) for the $Li_3AlB_2O_6$ and $LiSrBO_3$. The emission band of 530 nm makes a red shift and fluorescence decay time of 24.39 ns becomes smaller for the $Li_3AlB_2O_6$ in comparison with the emission band of 480 nm and lifetime of 93.16 ns for the $LiSrBO_3$ at the visible region. Finally, the transition energies and oscillator strengths of the clusters $(Li_3AlB_2O_6)_2$ and $(LiSrBO_3)_2$ lying at low excited states were calculated by the time-dependent Hartree-Fock

Table 4 The transition energies and oscillator strengths of some low excited states

No.	$Li_3AlB_2O_6$		$LiSrBO_3$	
	Energy/eV	Strength	Energy/eV	Strength
1	3.0646	0.0027	3.0313	0.0013
2	3.0990	0.0061	3.1517	0.0129
3	3.2686	0.0002	3.1917	0.0010
4	3.3156	0.0040	3.2945	0.0035
5	3.3594	0.0028	3.3507	0.0067
6	3.4402	0.0022	3.3545	0.0001
7	3.5081	0.0001	3.5013	0.0008
8	3.5224	0.0024	3.5049	0.0040
9	3.5540	0.0228	3.5529	0.0024
10	3.7148	0.0025	3.5771	0.0006

method. The obtained results were used to model the photophysical properties and discuss the assignments of spectral bands of the $Li_3AlB_2O_6$ and $LiSrBO_3$. To the best of our knowledge, it is the first time to report the luminescence originated from undoped borates.

References

1 Chen, C. Z.; Gao, D. S.; Chen, C. T. *Acad. Thesis Conf. Cryst. Growth Mater. (China)* **1979**, *B44*, 107.

2 Chen, C. T.; Wu, Y. C.; Jiang, A. D.; Wu, G.; You, M.; Li, R. K.; Lin, S. J. *J. Opt. Soc. Am.* **1989**, *B6*, 616.

3 Akella, A.; Keszler, D. A. *Mater. Res. Bull.* **1995**, *30*, 105

4 Diaz, A.; Keszler, D. A. *Mater. Res. Bull.* **1996**, *31*, 147

5 Sasaki, T.; Mori, Y.; Yoshimura, M.; Yap, Y. K.; Kamimura, T. *Mater. Sci. Eng., R* **2000**, *30*, 1.

6 Mori, Y.; Kuroda, I; Nakajima, S.; Sasaki, T.; Nakai, S. *Appl. Phys. Lett.* **1995**, *67*, 1818.

7 Hu, Z. G.; Higashiyama, T.; Yoshimura, M.; Yap, Y. K.; Mori, Y.; Sasaki, T. *Jpn. J. Appl. Phys.* **1998**, *37*, L1093.

8 He, M.; Chen, X. L.; Hu, B. O.; Zhou, T.; Xu, Y. P.; Xu, T. *J. Solid State Chem.* **2002**, *165*, 187.

9 Abdullaev, G.; Mamedov, K. *Kristallografiya* **1974**, *19*, 165.

10 Abdullaev, G.; Mamedov, K. *Kristallografiya* **1982**, *27*, 381.

11 He, M.; Chen, X. L.; Gramlich, V.; Baerlocher, C.; Zhou, T.; Hu, B. Q. *J. Solid State Chem.* **2002**, *163*, 369.

12 Koskentalo, T.; Leskela, M.; Niinisto, L. *Mat. Res. Bull.* **1985**, *20*, 265.

13 Verstegen, J. M. P. J. *J. Electrochem. Soc.: Solid-State Sci. Technol.* **1974**, *121*, 1631.

14 Cheng, W. D.; Zhang, H; Lin, Q. S.; Zhang, Q. E.; Chen, J. T. *Chem. Mater.* **2001**, *13*, 1841.

15 Sheldrick, G. M. *SHELXS-97, Program for X-ray Crystal Structure Solution*, Göttingen University, Germany, **1997**.

16 Sheldrick, G. M. *SHELXS-97, Program for X-ray Crystal Structure Refinememt*, Göttingen University, Germany, **1997**.

17 Stevens, W. J.; Kraus, M.; Basch, H.; Jasin, P. G. *Can. J. Chem.* **1992**, *70*, 612.

18 Cundari, T. R.; Stevens, W. J. *J. Chem. Phys.* **1993**, *98* 5555.

19 Pople, J. A.; Frisch, M. J.; Trucks, G. W.; Schlegel, H. B.; Scuseria, G. E.; Robb, M. A.; Cheeseman, J. R.; Zakrzewski, V. G.; Montgomery, J. A.; Stratmann, R. E.; Burant,J. C.; Dapprich, S.; Millam, J. M.; Daniels, A. D.; Kudin, K. N.; Strain, M. C.; Farkas,O.; Tomasi, J.; Barone, V.; Cossi,M.; Cammi, R.; Mennucci, B.; Pomelli, C.; Adamo, C.; Clifford, S.; Ochterski, J.; Petersson, G. A.; Ayala, P. Y.; Cui, Q.; Morokuma, K.; Malick, D. K.; Rabuck, A. D.; Raghavachari, K.; Foresman, J. B.; Cioslowski, J.; Ortiz, J. V.; Stefanov, B.; Liu, B. G.; Liashenko, A. P.; Piskorz, I.; Komaromi, R.; Gomperts, R. L.; Martin, D. J.; Fox, T.; Keith, M. A.; Al-Laham, C. Y.; Peng, A.; Nanayakkara, C.; Gonzalez, M.; Challacombe, P. M.; Gill, W.; Johnson, B. G.; Chen, W.; Wong, M. W.; Andres, J. L.; Head-Gordon, M.; Replogle, E. S.; Gaussian, Inc., Pittsburgh PA, **1998**.

20 Gajhede, M.; Larseb, S.; Rettrup, S. *Acta Crystallogr. Sect. B: Struct. Sci.* **1986**, *C42*, 545.

(E0305199 ZHAO, X. J.)